Journal of Applied Polymer Science

Antisolvent crystallization and solid-state polymerization of bisphenol-A polycarbonate

Xuesong Chang, Tongmei Ding, Hengshui Tian, Tiantian Wang
School of Chemical Engineering, East China University of Science and Technology, Shanghai 200237, People's Republic of China
Correspondence to: H. S. Tian (E-mail: hstian@ecust.edu.cn)

ABSTRACT: Bisphenol-A polycarbonate (BAPC) was synthesized by solid-state polymerization (SSP) using a semicrystalline prepolymer crystallized by antisolvent method. The antisolvent crystallization was investigated as a function of antisolvent types using X-ray diffraction (XRD), different scanning calorimetry (DSC), and scanning electron microscopes (SEM). The results showed antisolvent types had a significant effect on the crystallization of BAPC. Prepolymer induced by acetone as an antisolvent gained a higher crystallinity of 37.0%, more uniform particle size, and mature crystal structure compared with the samples crystallized by methanol and ethanol. Then crystallization of BAPC by acetone was carried out at crystallization temperature in the range of 40–80 °C for 1–5 h. A high crystallinity of 42.0% was acquired with the crystallization conducted at 70 °C for 2 h. Prepolymer with appropriate crystallinity of 37.8% resulted in high-molecular-weight polymer of 57,411 via SSP due to the effect of crystallinity and plasticization of residual solvent. © 2016 Wiley Periodicals, Inc. J. Appl. Polym. Sci. **2016**, *133*, 43636.

KEYWORDS: crystallization; polycarbonates; polycondensation

Received 25 November 2015; accepted 10 March 2016
DOI: 10.1002/app.43636

INTRODUCTION

Bisphenol-A polycarbonate (BAPC) is a polymer with remarkable properties, such as excellent optical transparency, toughness, heat resistance, creep resistance, processability, and antiweatherability.[1–3] Industrially, BAPC is synthesized either by interfacial phosgenation of bisphenol-A (BPA) with phosgene or by melt polymerization of BPA with diphenyl carbonate (DPC).[4] BAPC with high molecular weight and high quality could be produced by interfacial phosgenation. However, organic and aqueous wastes, which could cause serious environmental problems, are generated during this process. Melt polymerization is an alternative environmentally benign route for polycarbonate production. The main drawback of melt polymerization process arises from the high viscosity of the melt, which limits removal of phenol, and also restricts the obtainable molecular weight of BAPC. High temperature subserves the melt reaction but increases side reaction rate, and it results in low-quality product with poor optical quality.[5]

Solid-state polymerization (SSP) is a pathway to obtain high molecular weight at a relatively low reaction temperature. The molecular weight of BAPC prepolymer particles synthesized by melt polymerization process further increases under vacuum or inter gas flow conditions at a temperature between the glass transition temperature ($T_g = 145$ °C) and melting temperature ($T_m = 220$–230 °C) of the prepolymer.[6] In SSP of BAPC, the amorphous prepolymer should be crystallized before the reaction; otherwise, the amorphous prepolymer particles would stick together and fuse to form a very viscous mass at the reaction temperature.[7]

The crystallinity of polymers depends on the chain flexibility. BAPC presents poor crystallization ability for the rigidity.[8,9] Even if BAPC has the crystalline ability, the thermal crystallization of BAPC is time-consuming. The first crystallization requires 24 h at a temperature higher than 200 °C, and a well-developed crystalline structure needs 1 week.[10–13] Several studies of different methods including solvent-induced crystallization,[14] vapor-induced crystallization,[9,15] supercritical CO_2-induced crystallization,[16–22] thin-film crystallization,[23,24] and vacuum process crystallization[8,25] to crystallize BAPC were reported. Fan *et al.*[15] studied vapor-induced crystallization of BAPC pellets by being exposed to acetone at 25 °C and 28 kPa. The results showed that crystallinity attained a maximum value of 17% when the exposure time was longer than 16 h. Ata *et al.*[24] investigated the crystallization of BAPC in spin cast thin film. It was found that high crystallinity was observed for 30-nm-thick film after annealing under vacuum at 200 °C for 48 h. Gross *et al.*[19] explored the crystallization of BAPC facilitated by supercritical CO_2 and a maximum induced crystallinity of approximately 25% was acquired at 20.4 mPa and 70 °C for 12 h. Therefore, these studies required high demand of apparatus (high vacuum or high pressure) and long time.

Liquid antisolvent processes are based on two completely miscible liquid solvents. The micronized solute can dissolve in the first solvent, but not in the second solvent. Therefore, the addition of antisolvent to a concentrated solution induces the supersaturation and the precipitation of the solute through the solubility reduction in the combined solvent mixture, which leads to crystallization.[26–29] Liquid antisolvent technology is traditionally used in micronization process of polymers such as poly(L-lactide), polyamides, polystyrene, and polyacrylonitrile.[30] However, to our best knowledge, few studies of liquid antisolvent method in BAPC crystallization were reported in the past decades. BAPC crystallization by liquid antisolvent is less time-consuming and simpler without high demand of apparatus. Moreover, it is possible to completely micronize BAPC prepolymer particle possessing constant particle distribution without grinding, which is favorable for SSP process.

In this work, crystallization of BAPC by antisolvent and SSP of semicrystalline BAPC prepolymers were investigated. The effects of antisolvent types, crystallization temperature, and crystallization time on crystallinity and molecular weight of solid-state-polymerized BAPC were studied and discussed.

EXPERIMENTAL

Materials

BPA (>99.8%) purchased from Xinchang Chemical (Taiwan, China) and DPC (>99.0%) manufactured by Yuanji Chemical (Shanghai, China) were employed as raw materials of BAPC prepolymer. DPC was crystallized by ethanol–water solution (21:9 by weight) and dried under vacuum at 50 °C prior to use. Tetraethyl ammonium hydroxide (TEAH, 20% aqueous) was obtained from Alfa Aesar (Ward Hill, America). Dichloromethane (AR, >99.5%), methanol (AR, >99.5%), ethanol (AR, >99.5%), and acetone (AR, >99.5%) were supplied by Lingfeng Chemical (Shanghai, China). Chloroform (HPLC grade, J&K Scientific) was used as the mobile phase of gel permeation chromatography (GPC).

Prepolymer Synthesis

BAPC prepolymer was prepared by melt polymerization of DPC and BPA using TEAH as a catalyst. DPC (0.32 mol) and BPA (0.30 mol) were added into an agitated reactor and heated to 180 °C under N_2 atmosphere. After the monomers melted, 104 μL of TEAH (TEAH:BPA molar ratio = 5×10^{-4}) was injected and reaction temperature was increased to 210 °C. Pressure was reduced to 18 kPa and kept for 25 min followed with a further decrease to 10 kPa for 10 min. Finally, the reactor was heated to 260 °C and kept for 30 min under vacuum (<0.4 kPa) to remove phenol. The prepolymer with a starting weight average molecular weight (M_w) relative to the polystyrene standard of 13,243 g/mol and the polydispersity index (PDI) of 1.89 was cooled to room temperature and collected.

Prepolymer Crystallization by Antisolvents

The antisolvent crystallization of BAPC was studied as a function of antisolvent types (acetone, methanol, and ethanol). The samples were crystallized by different antisolvents at 50 °C for 2 h. The crystallization experiment was conducted as follows: 30 g BAPC prepolymer was dissolved in 100 mL dichloromethane. After BAPC dissolved completely, 100 mL antisolvent was added dropwise with vigorous stirring until the precipitate finished completely. The upper solvent was removed after the crystallization time (1–5 h), whereas the lower solution was evaporated at the desired temperature (40–80 °C) to remove the solvent. Finally, obtained particles were dried under vacuum at 50 °C for 2 h. In addition, neat BAPC prepolymers were ground to be a particle with the size of 60–80 mesh using a mortar and a pestle (or the grinder).

Solid-State Polymerization

SSP experiments were carried out with the crystalline prepolymer. Ten grams of semicrystalline particles with a certain size range (60–80 mesh) was added into the reactor after stabilizing reactor pressure. The reaction was carried out under vacuum at 210 °C for 8 h.

Characterization

Fourier transform infrared (FTIR) spectra, ranging from 4000 to 400 cm^{-1}, was conducted by a Nicolet 6700 spectrometer using thin films.

X-ray diffraction (XRD) was conducted on an ESCALAB250Xi. The instrument was operated at an excitation voltage of 40 kV and a current of 100 mA. The scanning 2θ ranged between 3° and 50° with a step scanning rate of 4°/min and the XRD spectra were recorded at a resolution of 0.02°.

Differential scanning calorimetry (DSC) measurements of crystalline BAPC samples were carried out on TA Q200-DSC calibrated with indium. Samples were dried under vacuum at 50 °C overnight prior to test, and weights of about 5 mg were used. Samples were heated from room temperature to 300 °C with liquid nitrogen with a heating rate of 10 °C/min. Glass-transition temperature (T_g) and melt temperature (T_m) were determined from an inflection point and the maximum point in the curve of melting endotherm, respectively. The heat of melting (ΔH_m) was obtained from the peak area of the melting endotherm. The degree of crystallinity (X_c) of BAPC was measured by the heat of melting and calculated by eq. (1):

$$X_c = H_m / H_f \times 100\% \quad (1)$$

Where H_m is the melting enthalpy of the sample and H_f is 26.2 cal/g or 110.4 J/g as the fusion heat of 100% crystallized PC according to ref. 31.

The morphology of the polymer crystals was investigated by NOVA Nano S-450 scanning electron microscopes (SEM). Polymer particle samples were coated with Au–Pd in a Denton vacuum evaporator.

GPC measurements were conducted at 25 °C on Waters 1525. The number (M_n) and weight (M_w) average molecular weights and the PDI of the polymers were measured. The mobile phase was chloroform with a flow rate of 1 mL/min. A GPC universal calibration curve was established using a viscosity detector and polystyrene standards.

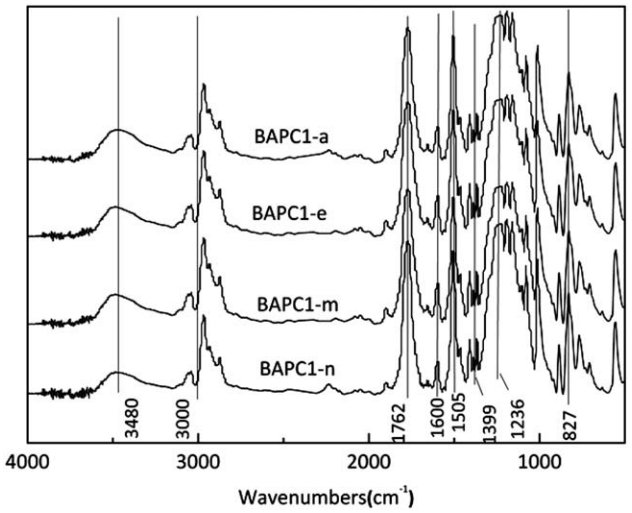

Figure 1. FTIR spectra of BAPC crystallized by different antisolvents.

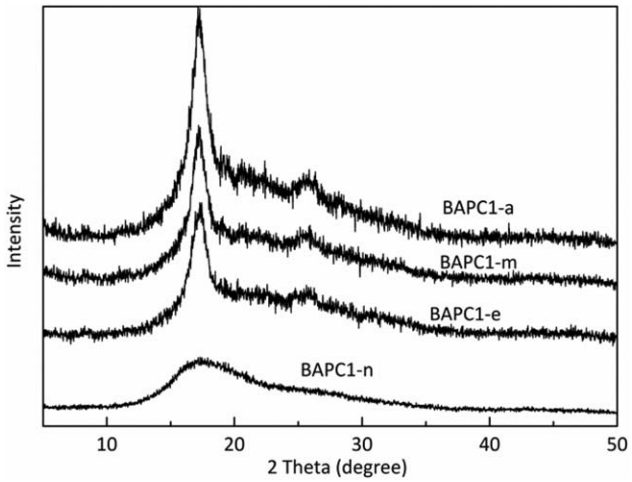

Figure 2. XRD patterns of BAPC crystallized by different antisolvents.

RESULTS AND DISCUSSION

Nomenclature Employed

The nomenclature used for this series is the form of BAPC*x*-*y*, where *x* equals the type of polymer (1 = prepolymer and 2 = SSP polycondensate) and *y* represents the antisolvent employed in the crystallization of BAPC (n = neat sample, a = acetone, m = methanol, and e = ethanol). For example, BAPC1-n is the prepolymer without any crystallization treatment.

FTIR Analysis

From the FTIR spectra of BAPC samples shown in Figure 1, the absorption bands around 3480 cm^{-1} belong to phenol end groups. The peaks above and below 3000 cm^{-1} are related to sp^2 carbon hydrogen and sp^3 carbon hydrogen stretching, respectively. The band at 1762 cm^{-1} could be ascribed to carbonyl stretching of the carbonate functional group, while the band at 1236 cm^{-1} is originated from C—O stretching vibration. Besides, the peaks at 1600 cm^{-1} and 1505 cm^{-1} correspond to C—C stretching and skeletal vibration of aromatic rings, as well as 827 cm^{-1} relates to C—H deformation vibration of aromatic ring. The weak double absorption peak of isopropylidene linkage at 1399 cm^{-1} is clearly distinguished. The results indicate that all antisolvents used do not change the structure of BAPC.

X-ray Diffraction

Figure 2 shows the diffraction patterns of crystallized samples (BAPC1-a, BAPC1-m, and BAPC1-e) in comparison with amorphous sample (BAPC1-n). BAPC1-n exhibited a broad diffraction peak, indicating that it was a totally amorphous sample. The crystallized samples showed a sharp reflection at 17.1°, suggesting the crystallization formation in these samples.

The results derived from XRD spectra are listed in Table I. The (020) reflections at $2\theta = 17.1°$ corresponded to the monoclinic unit cell and the values of 2θ were comparable to those obtained by Bonart.[32] Sample BAPC1-a showed a minimum half-height width ($\beta_{1/2}$) (1.31), implying that BAPC1-a had a larger size of crystal grain.[15] It was suggested that the solubility parameter, polarity, and hydrogen bond of various antisolvents had significant impacts on BAPC crystallization.[33] As the polarity and hydrogen bond of acetone, methanol, and ethanol were similar, the high crystallization ability of acetone could be due to the close solubility parameter of acetone (10.0) and BAPC (9.5), compared with those of methanol (14.7) and ethanol (12.7).[34]

DSC Measurements

Figure 3 collects the DSC scan of the BAPC samples. The results of T_g, T_m, H_m, and X_c are listed in Table II. As shown in Table II and Figure 3(a), T_g of crystallized samples were higher than the neat sample, indicating that the existence of crystal region restricted the chain mobility of amorphous region.[35] In addition, the T_g of crystallized samples were very close.

No obvious melting peak was observed for BAPC1-n in Figure 3(b), which could be connected with none crystallization in the neat sample.[18] In contrast, the DSC curves exhibited obvious endothermic peaks after antisolvent crystallization. T_m of samples BAPC1-a, BAPC1-m, and BAPC1-e were 244.3, 247.0, and 243.9 °C, respectively. The difference of T_m could be attributed to different lamellar thickness estimated from the Gibbs–Thomson equation.[23] Meanwhile, the broad melting peaks of BAPC1-m and BAPC1-e were suggested to the inhomogeneous lamellar thickness.[36] The crystallinity of BAPC1-a was maximum (37.0%), which was in accordance with XRD results.

SEM Morphology

SEM morphology of the polycarbonate particles for BAPC1-n, BAPC1-a, BAPC1-m, and BAPC1-e is shown in Figure 4.

Table I. XRD Data of BAPC Samples Crystallized by Different Antisolvents

Sample	2θ	$\beta_{1/2}$[a]
BAPC1-a	17.04	1.31
BAPC1-m	17.06	1.37
BAPC1-e	17.09	1.33

[a] The half-height widths of the 020 reflections.

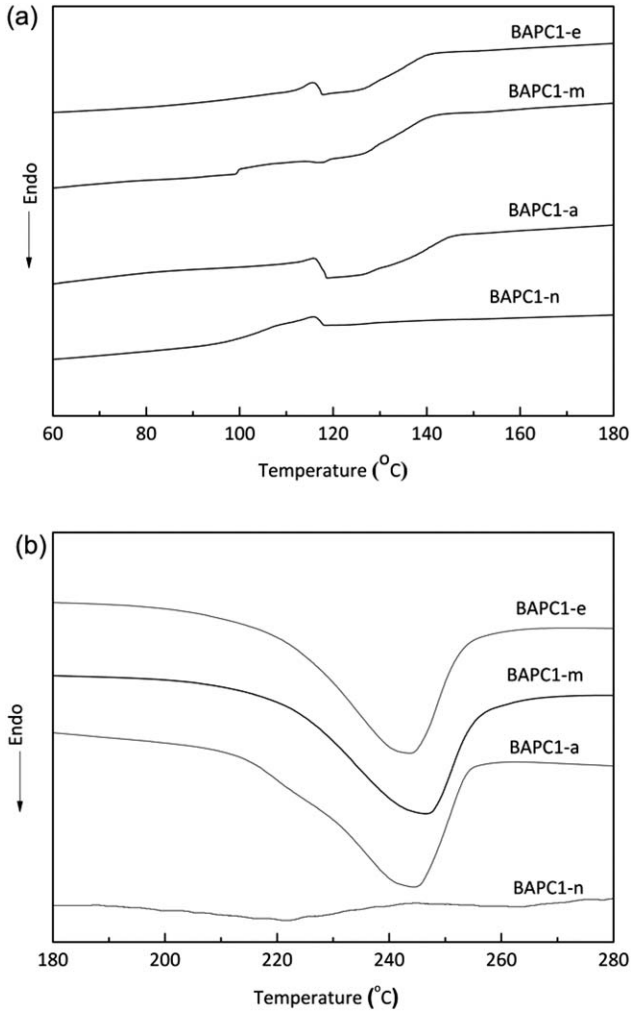

Figure 3. DSC curves of BAPC crystallized by different antisolvents.

It was obvious that the surface of neat BAPC was smooth at both high and low scales in Figure 4(a–d).

At the lower magnification, no polymer mass was present among the spherulitic polymer particles. BAPC1-a surface exhibited a hierarchical structure composed of microscale pores, spherulites, and fibrils. As can be seen in Figure 4(e), most of the spherulities in sample BAPC1-a took on the appearance of isolated ellipsoids in nearly uniform size (about 11–13 μm in diameter). In Figure 4(f), as the original amorphous polymer was penetrated by acetone, the original polymer mass in the BAPC sample was dragged toward the crystal nuclei to form polymer particle layer. Figure 4(g,h) shows the higher magnification of the spherulite characteristic group in Figure 4(f). A fine surface structure could be detected clearly on the mature spherulite. Meanwhile, the fibrils formed by lamellar structures were observed on the surface of the top layer of spherulites in Figure 4(h).

The polymer particles of BAPC1-m, in Figure 4(i), were not quite spherical but rather flat or hemispherical, suggesting that antisolvent methanol restricted the formation of fully developed three-dimensional spherulites. As seen in Figure 4(k,l), the interior structure of hemispherulites and needle-like crystals was observed on the surface with partially open structures. Meanwhile, some polymer mass were present among the spherulitic polymer particles, which indicated that crystallization occurred partially.

BAPC1-e in Figure 4(m) showed little near-planar (two-dimensional) spherulitic morphology, and irregular particles were present on the destroyed surface. Some fibrils and little polymer mass appeared at the lager magnification, indicating that crystallization by ethanol occurred rarely.

Compared with samples crystallized by methanol and ethanol, those crystallized by acetone showed more mature crystal structure and uniform spherulitic particles. This was in agreement with the results of DSC and XRD.

Molecular Weight of Prepolymers and Solid-State-Polymerized Polymers

SSP was carried out with the semicrystalline prepolymers (M_w = 13,243), and the results are summarized in Table III. The molecular weight of all crystalline prepolymers increased after SSP, which demonstrated that the use of antisolvents was compatible with the SSP of BAPC. And the molecular weight of BAPC2-a was much higher than those of BAPC2-m and BAPC2-e, which was ascribed to the higher crystallinity in BAPC2-a. Moreover, there was a slight change in the molecular weight of BAPC1-a, while the molecular weight of BAPC1-m and BAPC1-e decreased. This phenomenon might be attributed to the alcoholysis of carbonate linkage in methanol and ethanol, especially in methanol.[37,38]

It was suggested that types of antisolvent played an important role to the crystallization of BAPC.[39,40] The results of XRD, DSC, and SEM showed that crystallization of BAPC occurred by antisolvent crystallization. The sample crystallized by acetone as the antisolvent possessed high crystallinity, uniform particle size, and mature crystal structure due to the similar solubility parameter of acetone (10.0) and BAPC (9.5). High-molecular-weight polymer after SSP was acquired with prepolymer crystallized by acetone. The different molecular weights of SSP polymers should be ascribed to the different prepolymer crystallinity.[41–43] High initial prepolymer crystallinity may increase SSP rate by increasing the concentration of reactive end groups in the amorphous phase that were rejected from the crystalline phase, which led to a more effective impingement and reaction.

Table II. Results from DSC Curves of BAPC Prepolymer Crystallized by Different Antisolvents

Sample	T_g (°C)	T_m (°C)	H_m (J/g)	X_c (%)
BAPC1-n	133	-	-	-
BAPC1-a	133	244.3	40.8	37.0
BAPC1-m	134	247.0	34.0	30.8
BAPC1-e	134	243.9	35.3	32.0

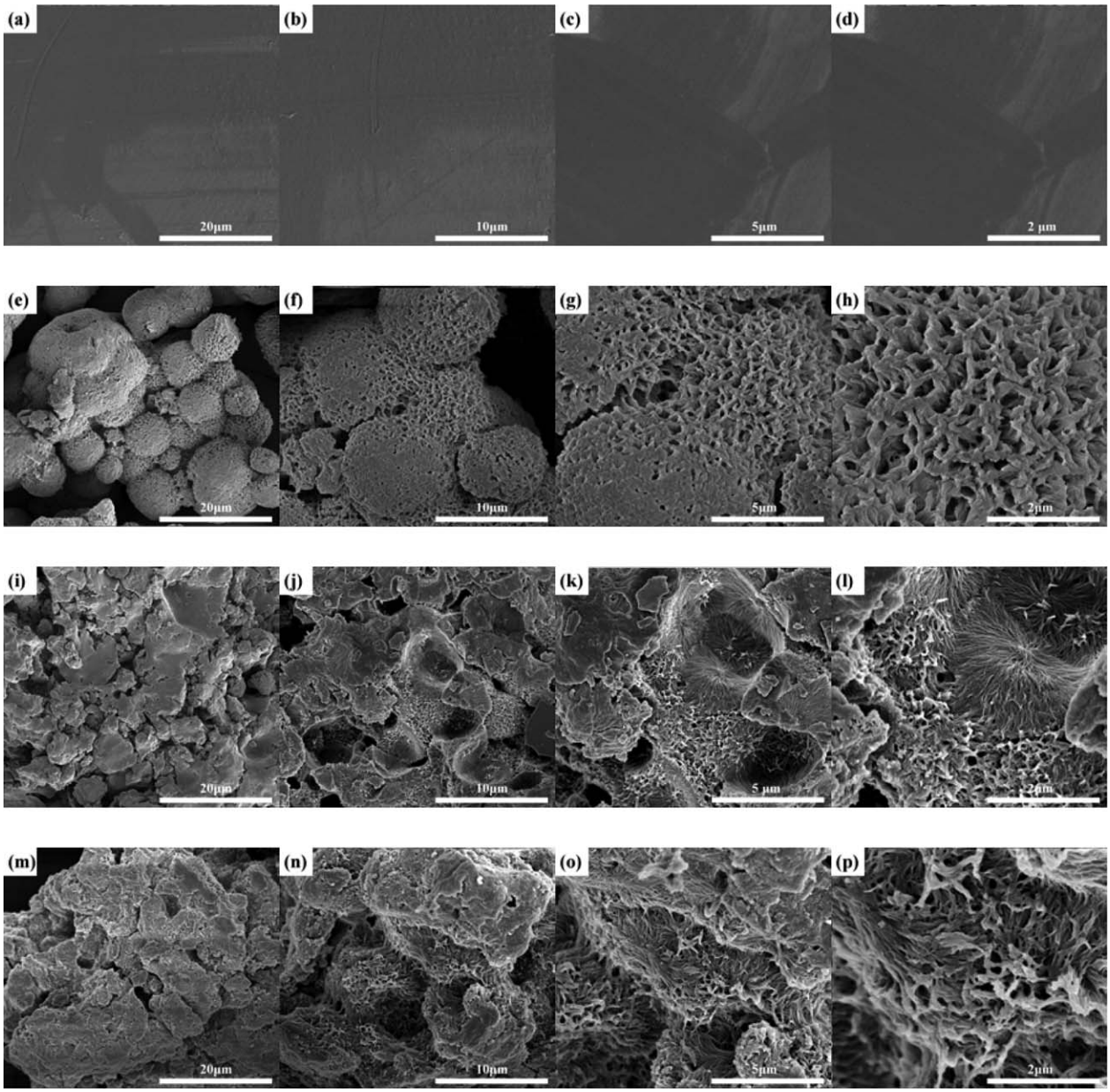

Figure 4. SEM of BAPC surfaces induced with different antisolvents across multiple length scales.

Effect of Crystallization Time on Crystallinity and SSP Polymer Molecular Weight

The DSC heating curves of BAPC crystallized by acetone at 50 °C with different crystallization time are shown in Figure 5. T_m increased with crystallization time and the difference in T_m of samples was about 10 °C. According to the study of Hu *et al.*,[20] the crystal-folding surfaces smoothed and the crystal developed as the crystallization time increased during isothermal crystallization, leading to the increase of T_m. Moreover, increasing regularity in the chain conformation at the crystal surface reduced the surface energy, therefore, resulted in the increase of T_m.

The crystallinity and molecular weight of BAPC crystallized by acetone at 50 °C with different crystallization time are shown in Figure 6. The results showed that the sample had a maximum induced crystallinity of approximately 40.0% at 3 h and maintained the asymptotic value to 5 h. The molecular weight increased sharply during the first 2 h with crystallinity increased

Table III. Molecular Weight of BAPC Crystallized by Different Antisolvents

Sample	M_w (g/mol)	Sample	M_w (g/mol)	PDI
BAPC1-n	13243	-	-	-
BAPC1-a	13230	BAPC2-a	57151	2.09
BAPC1-m	13010	BAPC2-m	45887	2.03
BAPC1-e	13132	BAPC2-e	50543	2.04

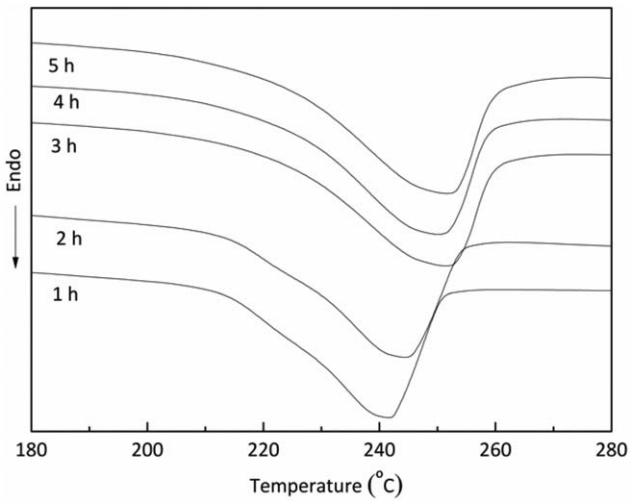

Figure 5. DSC curves of BAPC crystallized by acetone at 50 °C with different time.

to 37.1%, indicating the effect of high crystallinity on SSP reaction mentioned above. But the molecular weight decreased as the crystallinity increased above 39.5%. Higher crystallinity could decrease SSP rate by inhibiting the mobility of polymer chains in the amorphous phase and hindering the diffusion of by-product throughout the polymer particles.[44,45] As a result of crystallinity effect, BAPC prepolymer of 2 h crystallization time with crystallinity of 37.1% synthesized the highest molecular weight of 57,343 in SSP reaction.

Effect of Crystallization Temperature on Crystallinity and SSP Polymer Molecular Weight

A series of experiments were carried out to investigate the effect of different crystallization temperatures by acetone for 2 h on X_c and molecular weight of SSP polymer. The results are summarized in Figure 7. The crystallinity increased from 35.9% to 42.0% with the increase of the crystallization temperature, and then reached the maximum value of 42.0% at 70 °C. During the antisolvent crystallization process, small crystallites generated and grew gradually with time until impingements occurred.[46] The small crystallites were more active to impinge at high temperature than those at low temperature. Antisolvents enabled

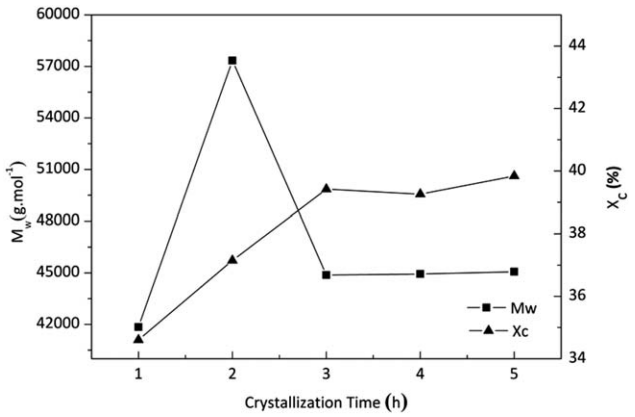

Figure 6. Crystallinity and molecular weight of BAPC crystallized by acetone at 50 °C with different crystallization time.

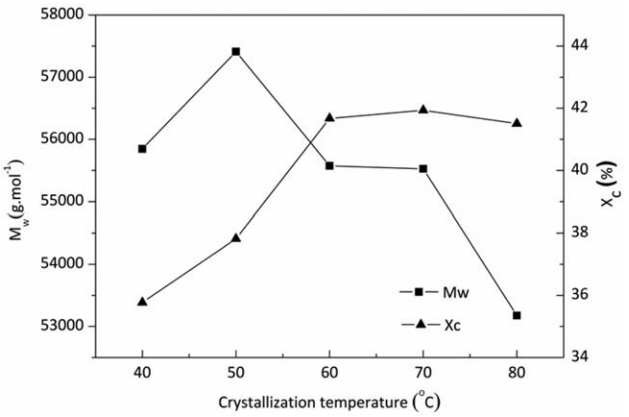

Figure 7. Crystallinity and molecular weight of BAPC crystallized by acetone at different temperature for 2 h.

this crystallization as it increased the free volume of the amorphous regions of the polymer at lower temperature. With the crystallization temperature increased to 80 °C, the smaller crystallites began to melt,[15] leading to the stable crystallinity.

The molecular weight of solid-state-polymerized BAPC increased with the increased crystallized temperature until 50 °C. Afterward, the molecular weight decreased sharply at 60–80 °C with the crystallinity of 41.5–42.0%. Besides the effect of crystallinity mentioned above, the plasticization agents such as solvent residues[47,48] also had an effect on the mobility of end groups. The plasticization increased the mobility of BAPC chains and enhanced the transport process between the amorphous and crystalline phases.[49–51] The increased chain and chain-segment mobility resulted in an increased SSP reaction rate and higher molecular weight of SSP polymer. As the crystallization temperature increased, the amount of absorbed solvent residues decreased. Therefore, the plasticization of solvent residues at high temperature was weaker than that at low temperature, which led to lower molecular weight in SSP.

According to the results mentioned above, two factors had an effect on the SSP reaction: the crystallinity and the solvent residues. As the contradictory effect of crystallinity and plasticization of solvent residues on the SSP reaction, high molecular weight of BAPC polymer could be acquired when the prepolymer with a crystallinity of 37.8% was solid-state polymerized in our study.

CONCLUSIONS

In summary, three-dimensional and uniform micrometer-scale semicrystalline BAPC spherulite from the amorphous polymer was prepared by antisolvent method. The effects of antisolvent types, crystallization time, and temperature on BAPC crystallization, as well as the effect of crystallinity and solvent residues on the molecular weight of SSP polymer, were investigated and discussed. The results showed that acetone was the most suitable antisolvent by comparison of crystal structure, crystallinity, and crystal morphology, leading to the maximum polymer molecular weight after SSP. A high crystallinity value (42%) of BAPC was acquired at 70 °C for 2 h by acetone. According to the contradictory effect of crystallinity and plasticization of

solvent residues, high-molecular-weight (57,411) BAPC would be synthesized by semicrystalline BAPC prepolymer with a crystallinity of approximately 37.8% during SSP reaction.

REFERENCES

1. Shi, C.; Desimone, J. M.; Kiserow, D. J.; Roberts, G. W. *Macromolecules* **2001**, *34*, 7744.
2. Colonna, M.; Berti, C.; Fiorini, M. *J. Appl. Polym. Sci.* **2013**, *131*, 39820.
3. Gross, S. M.; Bunyard, C.; Erford, K.; Roberts, G. W.; Kiserow, D. J.; Desimone, J. M. *J. Polym. Sci. A: Polym. Chem.* **2001**, *40*, 171.
4. Kim, Y.; Choi, K. Y. *Ind. Eng. Chem. Res.* **1992**, *31*, 2118.
5. Woo, B.; Choi, K. Y. *Ind. Eng. Chem. Res.* **2001**, *40*, 1312.
6. Vouyiouka, S. N.; Karakatsani, E. K.; Papaspyrides, C. D. *Prog. Polym. Sci.* **2005**, *30*, 10.
7. Ye, Y. S.; Choi, K. Y. *Ind. Eng. Chem. Res.* **2008**, *47*, 3687.
8. Mochizuki, H.; Mizokuro, T.; Tanigaki, N.; Hiraga, T.; Ueno, I. *Polym. Adv. Technol.* **2005**, *16*, 67.
9. Takahashi, T.; Yonetake, K.; Koyama, K.; Kikuchi, T. *Macromol. Rapid Commun.* **2003**, *24*, 763.
10. Falkai, B. V.; Rellensmann, W. *Macromol. Chem. Phys.* **1964**, *75*, 112.
11. Peilstöcker, G. *Br. Plast.* **1962**, *35*, 365.
12. Kambour, R. P.; Karasz, F. E.; Daane, J. H. *J. Polym. Sci. A2 Polym. Phys.* **1966**, *4*, 327.
13. Mercier, J. P.; Groeninckx, G.; Lesne, M. *J. Polym. Sci. C Polym. Symp.* **1967**, *16*, 2059.
14. Cui, Y. H.; Paxson, A. T.; Smyth, K. M.; Varanasi, K. K. 13th IEEE ITHERM Conference on superhydrophobic Polymer Surface via Solvent-induced Crystallization, Cambridge, MA, USA, **2012**, p 951.
15. Fan, Z.; Shu, C.; Yu, Y.; Zaporojtchenko, V.; Faupel, F. *Polym. Eng. Sci.* **2006**, *46*, 729.
16. Gedler, G.; Antunes, M.; Velasco, J. I. *Polymer* **2013**, *54*, 6389.
17. Li, G.; Park, C. B. *J. Appl. Polym. Sci.* **2010**, *118*, 2898.
18. Lu, J.; Xi, D. K.; Hung, R.; Li, L. B. *J. Macromol. Sci. Phys.* **2011**, *50*, 1018.
19. Gross, S. M.; Roberts, G. W.; Kiserow, D. J.; Desimone, J. M. *Macromolecules* **2000**, *33*, 40.
20. Hu, X. B.; Lesser, A. J. *Polymer* **2004**, *45*, 2333.
21. Liao, X.; Wang, J.; Li, G.; He, J. S. *J. Polym. Sci. B: Polym. Phys.* **2004**, *42*, 280.
22. Mascia, L.; Delre, G.; Ponti, P. P.; Bologna, S.; Giacomo, D. *Adv. Polym. Technol.* **2006**, *25*, 225.
23. Ye, Y. S.; Choi, K. Y. *Macromol. Mater. Eng.* **2009**, *294*, 847.
24. Ata, S.; Oka, T.; He, C. Q.; Ohdaira, T.; Suzuki, R.; Ito, K.; Kobayashi, Y.; Ougizawa, T. *J. Polym. Sci. B: Polym. Phys.* **2010**, *48*, 2148.
25. Mochizuki, H.; Mizokuro, T.; Tanigaki, N.; Ueno, I.; Hiraga, T. *J. Polym. Sci. B: Polym. Phys.* **2005**, *43*, 2307.
26. Sheikhzadeh, M.; Trifkovic, M.; Rohani, S. *Chem. Eng. Sci.* **2008**, *63*, 829.
27. Kitamura, M.; Sugimoto, M. *J. Cryst. Growth* **2003**, *257*, 177.
28. Guo, Z.; Zhang, M.; Li, H.; Wang, J.; Kougoulos, E. *J. Cryst. Growth* **2005**, *273*, 555.
29. O'Grady, D.; Barrett, M.; Casey, E.; Glennon, B. *Chem. Eng. Res. Des.* **2007**, *85*, 945.
30. Reverchon, E. *J. Supercrit. Fluids* **1999**, *15*, 1.
31. Mercier, J. P.; Legras, R. *J. Polym. Sci. B Polym. Lett.* **1970**, *8*, 645.
32. Bonart, R.; Hosemann, R.; Mccullough, R. L. *Polymer* **1963**, *4*, 199.
33. Moore, W. R.; Sheldon, R. P. *Polymer* **1961**, *2*, 315.
34. Kambour, R. P.; Gruner, C. L.; Romagosa, E. E. *Macromolecules* **1974**, *7*, 248.
35. Zhai, W.; Yu, J.; Ma, W.; He, J. *Macromolecules* **2007**, *40*, 73.
36. Yin, B.; Zhao, Y.; Yang, W.; Pan, M. M.; Yang, M. B. *Polymer* **2006**, *47*, 8237.
37. Pinero, R.; Garcia, J.; Cocero, M. J. *Green. Chem.* **2005**, *7*, 380.
38. Huang, J.; Huang, K.; Zhou, Q.; Chen, L.; Wu, Y. Q.; Zhu, Z. B. *Polym. Degrad. Stab.* **2006**, *91*, 2307.
39. Oosterhof, H.; Witkamp, G. J.; Van Rosmalen, G. M. *Fluid Phase Equilib.* **1999**, *155*, 219.
40. Takiyama, H.; Otsuhata, T.; Matsuoka, M. *Chem. Eng. Res. Des.* **1998**, *76*, 809.
41. Kim, J.; Kim, Y. J.; Kim, J. D.; Ahmed, T. S.; Dong, L. B.; Roberts, G. W.; Oh, S. G. *Polymer* **2010**, *51*, 2520.
42. Goodner, M. D.; Gross, S. M.; Desimone, J. M.; Roberts, G. M.; Kiserow, D. J. *J. Appl. Polym. Sci.* **2001**, *79*, 928.
43. Goodner, M.; Desimone, J. M.; Kiserow, D. J.; Roberts, G. R. *Ind. Eng. Chem. Res.* **2000**, *39*, 2797.
44. Baughman, R. H. *J. Polym. Sci. Polym. Phys. Edi.* **1974**, *12*, 1511.
45. Baick, I. H.; Ye, Y.; Luciani, C. V.; Ahn, Y. G.; Song, K. H.; Choi, K. Y. *Ind. Eng. Chem. Res.* **2013**, *52*, 17419.
46. [Aharoni, S. M.; Murthy, N. S. *Int. J. Polym. Mater.* **1998**, *42*, 275.
47. Ye, Y. S.; Machado, B.; Choi, K. Y. *Ind. Eng. Chem. Res.* **2005**, *44*, 2494.
48. Iyer, V. S.; Sehra, J. C.; Ravindranath, K.; Sivaram, S. *Macromolecules* **1993**, *26*, 1186.
49. Colonna, M.; Fiorini, M. *Polym. Eng. Sci.* **2015**, *55*, 1024.
50. Aharoni, S. M.; Murthy, N. S. *J. Polym. Mater.* **1998**, *42*, 275.
51. Wyzgoski, M. G.; Yeh, G. S. Y. *Int. J. Polym. Mater.* **1974**, *3*, 133.